

# Beam-plasma interaction in the ITER NBI

A. Lifschitz<sup>1</sup>, F. Dure<sup>1</sup>, G. Maynard<sup>1</sup>, J. Bretagne<sup>1</sup>, A. Simonin<sup>2</sup>, T. Minea<sup>1</sup>

1) Laboratoire de Physique des Gaz et Plasmas (LPGP), Université Paris Sud XI, Bat. 210, 91405 Orsay Cedex, France

2) DRFC, CEA Cadarache, 13108 Saint-Paul lez Durance, France

E-mail contact of main author: Agustin.Lifschitz@u-psud.fr

**Abstract** In the neutraliser of the ITER Neutral Beam Injector, a beam of negative ions ( $D^-$ ) of about 1 MeV passes through a structure filled with deuterium gas, where negative ions are mainly converted into fast atoms. The ionisation of the deuterium buffer gas filling the neutraliser induced by the  $D^-$  beam creates a rarefied and low temperature plasma which screens the electrostatic well of the  $D^-$  beam and affects the properties of the extracted beam and the energy transport to the neutraliser walls. Moreover, the plasma can eventually escape from the neutraliser and move back in the accelerator, toward the accelerating grids and the negative ion source. The OBI-2 (Orsay Beam Injector 2 dimensional) code was developed to simulate the beam propagation and plasma formation. Particle-particle and particle-wall collisions are treated using the Monte Carlo collision approach and the plasma is treated via Particle-in-Cell. The neutraliser geometry has been chosen as cylindrical with volume to surface aspect ratio representative of real technical devices designed for ITER neutral beam heating. Simulations show that the secondary plasma effectively screens the beam space charge preventing beam radial expansion induced by the Coulomb repulsion between beam ions. Plasma ions created in the neutraliser form an upstream current impinging the accelerator grid. On the other hand, the presence of these plasma ions between the accelerator grids and the neutraliser entrance enhances the beam focusing.

## 1. Introduction

The Tokamak plasma certainly needs additional heating for its ignition because the Joule heating efficiency decreases with the plasma temperature. Moreover, the maximum value of the plasma current is limited by the onset of magnetohydrodynamic instabilities that kill the discharge (disruption). There are basically two ways of increasing the energy content of the plasma: injecting either highly energetic particles or the plasma particle acceleration by resonant absorption of electromagnetic field. In both cases the energy must be transferred to the bulk of the plasma and, ultimately to the fuel-ion component to generate the fusion reactions.

In the future experimental fusion reactor ITER, to achieve thermonuclear fusion conditions the heating of plasma ions will be performed through the injection of energetic neutral ( $D^0$ ) beams. The two Neutral Beam Injectors (NBI) designed for ITER should bring a power of about 35 MW.  $D^0$  atoms must have about 1 MeV inside the Tokamak chamber.

Each NBI is composed by four parts: the negative ion source (40 A of  $D^-$ ), the accelerator (1 MV single gap or multi-grid), the neutralizer (for the conversion of  $D^-$  in  $D^0$ ), and the ion deflector (for the removal of charged particles remaining in the beam at its exit from the neutralizer,  $\sim 20\%$   $D^-$  and  $\sim 20\%$   $D^+$ ). The neutraliser is crucial for the final NBI performances, because the beam transport taking place there will determine ultimately the neutral beam properties just before entering the ITER confining chamber.

The present modeling work was undertaken to evaluate the efficiency of the NBI in terms of negative ion beam conversion into neutrals and beam geometrical properties at extraction for several designs using the recently developed numerical tool OBI-2 (Orsay Beam Injector, two dimensional code). The ionization induced by the  $D^-$  beam on the buffer gas ( $D_2$ ) filling the

neutraliser creates a rarefied residual low-temperature plasma. The role and dynamics of the residual plasma will also be treated. This plasma can screen the electrostatic well of the D<sup>-</sup> beam and, consequently, affect the properties of the extracted beam emittance and the energy transport to the neutraliser walls.

In this paper we present our numerical simulation results of the beam and plasma behaviour in the neutraliser for the Neutral Beam Injector (NBI) system of ITER. New physical problems appear that we address hereafter. One of them is the evolution of the buffer gas state due to its interaction with the energetic beam particles and the influence of this evolution on the beam transport. We especially investigated the ionisation of the buffer gas atoms creating a secondary plasma which expands in both directions, axial and transverse. Because we are dealing with very long pulses duration, the plasma can expand well outside the neutraliser. In particular it can reach the acceleration grids and possibly perturb the acceleration field.

The aim of the present study is to investigate the formation of this secondary plasma and to get an accurate knowledge of its characteristics, i.e. potential, charged particle density, electron temperature, etc.

## 2. Numerical approach and elementary processes

The Particle-In-Cell OBI-2 (Orsay Beam Injector – 2 dimensional) code was developed especially to answer the questions concerning the beam and plasma behaviour inside the ITER negative ion neutraliser. It originates from a previous code developed at LPGP and LBNL for heavy ion inertial fusion application [1, 2, 3]. It deals with a beam of energetic ions (H<sup>-</sup> or D<sup>-</sup> of given energy and current density) that crosses through a gaseous target (H<sub>2</sub> or D<sub>2</sub> of given density profile). To describe both the plasma expansion along the beam axis ( $z$ ) and the diffusion field in the radial direction ( $r$ ) we have considered a 2D ( $r,z$ ) axi-symmetrical system. In this model, the neutraliser copper plates are substituted by a tube.

The mean free paths of the plasma particles are of the same order of magnitude as the dimensions of the neutraliser. Therefore the transport is non-local, the plasma is not in equilibrium and collisions with the walls have a large contribution.

The **OBI-2** code includes atomic collisions through Monte Carlo Collision (MCC) approach. The code was upgraded to speed on calculations. The physical model included in the code was also improved to allow a detailed description of the induced residual plasma created by collisions between the beam particles and gas atoms and molecules. The geometry of the neutraliser used in the present work consist of a 2D cylindrical symmetry which is not the actual configuration of the neutraliser plates, but remains realistic in terms of the volume to surface aspect ratio. Hence, it is possible to follow the residual plasma formed between the symmetry axis and the wall but also forward and backward along the beam axis. Therefore, the simulation results here reported are electrostatic, in  $2^{1/2}$  dimensions ( $r,z,v_x,v_y,v_z$ ).

The main features of the OBI-2 code are given below. Details can be found in Ref [4].

- 1) The collision module takes account of the real physical situation through the main interaction processes present in the neutraliser. The code deals with elastic and inelastic collisions with arbitrary number of produced particles and multiple differential cross sections. The used MCC method is of the highest efficiency for reactions where only one of the colliding particles is modified during the collision, it has been generalized to treat also more general types of collisions such as charge exchange.

In OBI-2 code the various fields (scalar or vectorial) are projected on a 2D grid, whereas the particle dynamics are obtained by integrating the macro-particles equations of motion. Atomic collisions are considered as stochastic processes that can either change the state of a macro-particle or create / destroy macro-particles. The projection over the grid of higher orders of the energy distribution or the energy spectrum is currently being implemented. This improve the description of the reactions for non-thermalized species.

2) The wall collision module has been extended in order to include the secondary electron emission induced by several types of particles and the neutralization and re-injection of ions impinging the wall.

3) An electrostatic module has been added. Full electromagnetic simulations have shown that retarded field effects are very small and also that the magnetic field produced by the beam itself does not affect significantly the plasma properties. Therefore, the Maxwell equations can be treated within the electrostatic approximation solving Poisson's equation. The bi-conjugate gradient algorithm was used to solve it. This module strongly improved the computing efficiency. Time steps of one order of magnitude larger than in the initial electromagnetic version are now used.

4) The particle initialization module now allows for injecting a continuous flow of particles in the simulation box. The buffer gas density and temperature is assumed to be stationary.

We consider incoming beam particles consisting of 1 MeV D<sup>-</sup> ions. The relevant atomic collision processes involved in the interaction of the beam particles with the buffer gas are summarized in Tables 1. It gives the reactions changing the state of the beam particles. They follow a previous modelling work performed by E. Surrey [5] who considered the conversion of negative ions into fast neutrals or positive atomic ions giving three beam components.

One can see in Table 1 that the stripping reaction (reaction 1) is the most efficient. Neutralisation of the negative ion beam is due mainly to this reaction which is at the origin of the fast neutral atoms composing the neutral beam. The corresponding cross section is  $\sigma_1 = 1.13 \text{ in } 10^{-16} \text{ cm}^2 \text{ units at } 500 \text{ keV/amu}$ .

Table 1 – Collision processes considered by E. Surrey [5]. The beam particles are bold faced.

	<i>Projectile</i>	<i>Target</i>	<i>Products</i>			$\sigma \text{ (x}10^{-16} \text{ cm}^2\text{)}$ <b>at 500 keV/amu</b>
1	<b>D<sup>-</sup></b>	D <sub>2</sub>	<b>D<sup>o</sup></b>	D <sub>2</sub>	<b>e_strip</b>	1.133
2	<b>D<sup>-</sup></b>	D <sub>2</sub>	<b>D<sup>+</sup></b>	D <sub>2</sub>	<b>2(e_strip)</b>	0.073
3	<b>D<sup>o</sup></b>	D <sub>2</sub>	<b>D<sup>+</sup></b>	D <sub>2</sub>	<b>e_strip</b>	0.38

The second important reaction is known as ‘neutral stripping’, labelled 3 in Table 1. It leads to the conversion of the fast neutral atoms into positive ions. This reaction requires at least two collisions during the beam cross through the neutraliser (first the formation of D<sup>o</sup> – reaction 1 – and second its conversion in D<sup>+</sup>). Besides, this reaction limits the amount of the fast neutrals available at the exit of the neutraliser. The corresponding cross section at 500 keV/amu is  $\sigma_3 = 0.38 \times 10^{-16} \text{ cm}^2$ .

In our velocity regime, ‘double stripping’ (Reaction 2) has a small cross section. Its efficiency is only a few percent of the simple stripping (Reaction 1) and the corresponding cross section is  $\sigma_2 = 0.073 \times 10^{-16} \text{ cm}^2$  [6].

Taking into account the reactions of Table 1, it is easy to derive an analytical expression for the relative populations of the three species composing the high energy beam  $D^-$ ,  $D^0$  and  $D^+$  in terms of the gas linear density interacting with  $D_2$  deuterium gas. Note that due to the low value of the gas density, excitation of  $D^0$  has no influence on the beam particles state because the de-excitation rates are much higher than the ionisation one. For this value we obtained 55.3 % of  $D^0$ , 18.5 % of  $D^-$ , and 26.2% of  $D^+$ . These values are very close to the previous estimation of the beam composition at the exit plane of the neutraliser.

Beside the collisions reported in Table 1, there are other reactions with the beam particles with significant cross sections at  $\sim 1$  MeV, which do not change the beam particle state but which can ionize the buffer gas molecules; these processes are summarized in Table 2.

Table 2 – Additional collision processes introduced in the PIC-MC simulation

	<i>Projectile</i>	<i>Target</i>	<i>Products</i>			$\sigma$ ( $\times 10^{-16}$ cm <sup>2</sup> ) at 500 keV/amu [7]
4	$D^+$	$D_2$	$D^+$	$D_2^+$	e	0.71
5	$D^0$	$D_2$	$D^0$	$D_2^+$	e	0.43
6	$D^-$	$D_2$	$D^-$	$D_2^+$	e	$\sigma_5 + \sigma_7 = 1.04$

Table 3 – Main stripped electron collision processes

	<i>Projectile</i>	<i>Target</i>	<i>Products</i>			$\sigma$ ( $\times 10^{-16}$ cm <sup>2</sup> ) at 272 eV [8]
7	<b>e_strip</b>	$D_2$	e	$D_2^+$	e	0.61
8	<b>e_strip</b>	$D_2$	<b>e_strip</b>	$D_2$		0.023

Electrons created through ionisation of the beam particles (Reaction 1-3), named stripped electrons, born with a velocity close the beam particles one, corresponding kinetic energy being 272eV. On the other hand, the electrons coming from the ionisation of the buffer gas molecules have a broad energy distribution so that one has to consider these electrons (Reactions 4, 5, and 6, Table 2) over a large range of energy from 15 eV up to about 1 keV. Reaction 7 from Table 3 concerns non-dissociative ionisation, which at 272 eV has a cross section  $\sigma_7 = 0.61 \times 10^{-16}$  cm<sup>2</sup>. Plasma electrons from the high energy tail of the distribution are also able to ionise the buffer gas. Stripped electrons can be elastically scattered when colliding with the buffer gas molecules (Reaction 8 - Table 3). This does not change the energy but rather induces an angular dispersion of the beam electrons. Due to the geometry of the neutraliser, this reaction plays an important role for the isotropisation of the secondary plasma; moreover even a small transverse diffusion can increase significantly the flux of particles on the neutraliser plates.

At the present stage of the model development, the secondary plasma involves only one positive ion species, the molecular ion  $D_2^+$  and two distinct electron populations: (i) stripped electrons, which are characterized by an energy around 272 eV when they leave the negative ions from the beam; and (ii) secondary electrons, which are produced by the residual gas ionization with an average energy of about 10 eV. As presented in the next section, this simplified kinetic scheme is able to build up the dense secondary plasma.

Reactions 4-7 yield the source term of the secondary plasma. To describe the evolution of this plasma it is also necessary to consider the main collision processes. A detailed description of the full chemical kinetics of the deuterium plasma can be found in Ref [9]. Looking at the dominant process and taking a typical value of  $10^{-16} \text{ cm}^2$  for the cross sections inside the plasma, we get a mean free path of the order of 100 cm, which is one order of magnitude larger than the distance between two neutraliser plates. Therefore, beside the source term, the most important collision processes are the interaction of the plasma particles (electrons and ions) with the walls. In this preliminary study the unaddressed processes have been neglected.

### 3. Simulation results

We present in this section results obtained with OBI-2 code taking into account the microscopic processes described in the previous section.

Let us first give an estimation of the current density transported by one beamlet of the negative ion source of ITER. The total current should be 40 A distributed over 1280 beamlets. Therefore the current of one beamlet is 31 mA for a beam diameter of about 12 mm (cross section  $\sim 1.1 \text{ cm}^2$ ), with a corresponding current density of  $\sim 28 \text{ mA/cm}^2 = 280 \text{ A/m}^2$ . In our simulation we use a 2D (r,z) geometry, assuming the neutraliser as a tube. The value of its diameter has been fixed at 100 mm, the real distance between the plates. Hence, assuming that the negative ion beams enter the neutraliser only in a disc of 80 mm diameter (a zone without beam of  $\sim 10 \text{ mm}$  is assumed close to the walls in order to limit the beam-wall interaction), our simulation domain corresponds to  $\sim 10$  beamlets (Fig. 1). The beam is focussed with a focal distance of 10 m in front of the acceleration grid.

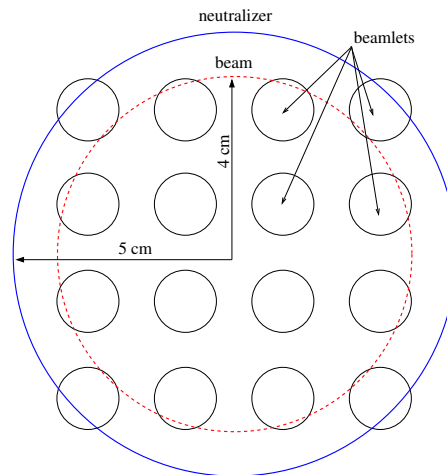


*Figure 1 – Beamlets entering the neutraliser cross section assuming the specification of the acceleration grid. Dot line disc sketches the broad uniform beam of 80 mm diameter composed of about 10 individual merged beamlets.*

Gas profile corresponds to 2 baffles cryogenic pumps at the end of the neutraliser and RID, with capture coefficient of 0.2 as calculated by Dr. Matthias Dremel, Forschungszentrum Karlsruhe [10]. This profile allowed us to extend the simulation box rearward the beam (starting from the acceleration grid) and forward joining the RID enter plane (6 m system length).

Let us remember that the first computation results using OBI-2 reported in [4] were limited to the neutraliser region only (3 m long cylinder). They did not take account of the particle transport from the accelerating grid to neutraliser entrance.

The present extended version can address all the processes over the simulated volume (6 m long and 10 cm diameter) and their associated effects are discussed below.

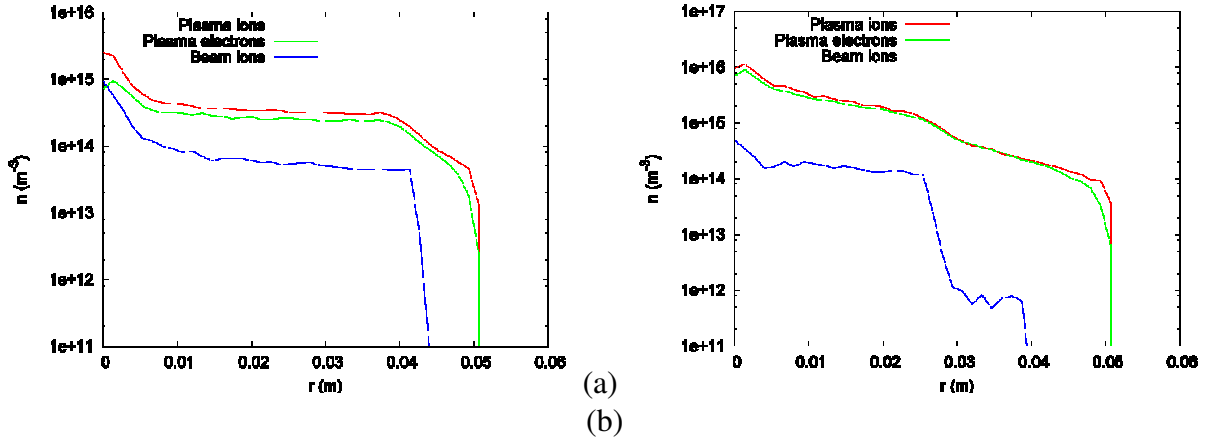


Figure 2 – Radial profiles of charged particles at the midplane of the neutraliser ( $z=3.5$  m) at (a)  $t = 1.4 \mu\text{s}$  and (b)  $20 \mu\text{s}$ .

At the early time of the simulation ( $1.4 \mu\text{s}$  – Fig; 2 (a) ), the beam diverges ( $r > 40$  mm) and the secondary plasma space charge is building-up. Later at  $20 \mu\text{s}$  (Fig. 2 (b) ), the quasi-neutral plasma fills almost all the neutraliser volume (the sheath thickness is  $< 10$  mm).

However at the same moment ( $1.4 \mu\text{s}$ ) after the beam enters in the neutraliser, the secondary plasma density is higher than the beam one. Hence, the neutralisation of the negative space charge starts helping the beam focusing. Approaching the steady-state ( $\sim 20 \mu\text{s}$ ), the secondary plasma density is almost one order of magnitude higher than the beam one (Fig. 2 (b) ). Consequently, the density gradient is much lower, especially at the beam border.

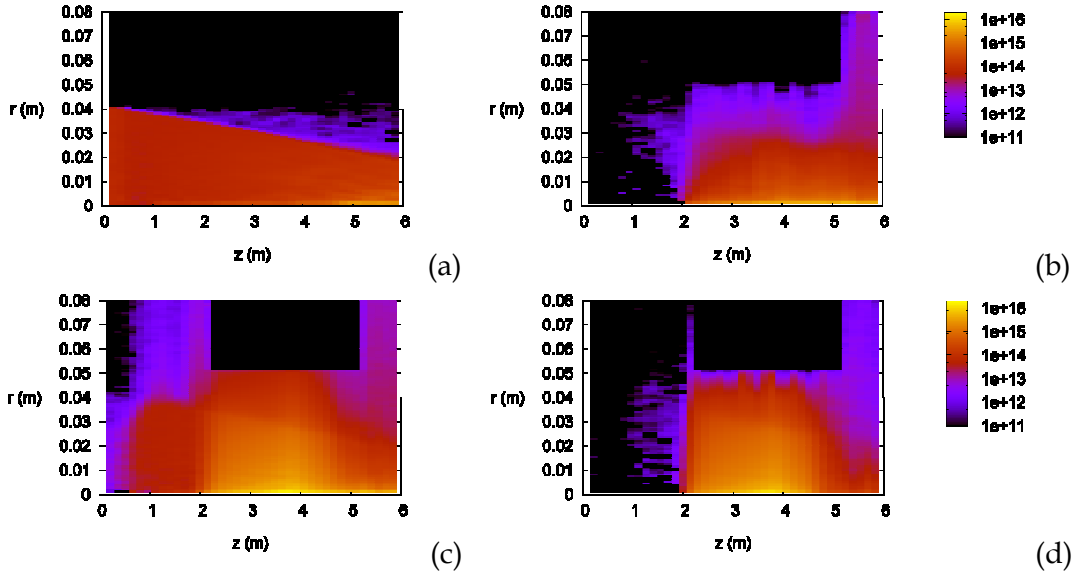


Figure 3 – Density distribution of beam and plasma particles at  $t = 20 \mu\text{s}$ , on logarithmic scale ( $\text{m}^{-3}$ ). (a) beam heavy species ( $D^-$ ;  $D^0$ ,  $D^+$ ); (b) stripped electrons; (c)  $D_2^+$  secondary plasma ions; (d) 'thermalized' plasma electrons.

Fig. 3 (a) shows, as expected, the beam radius decreasing with  $z$  due to the beam focusing. At the neutraliser midplane ( $z = 3.5$  m), the beam radius is  $\sim 25$  mm (blue line – Fig. 2 (b) ).

The charge beyond this radius ( $r > 25$  mm,  $n \sim 10^{12}$  m<sup>-3</sup>) corresponds to the halo due to particles neutralised inside the accelerator.

From the 2D ( $r,z$ ) density distributions shown in Fig. 3 at 20  $\mu$ s we can observe that the beam focusing follows the input angle and appears unaffected by the own negative space charge (Coulomb repulsion induces beam divergence). The initial trajectories are preserved due to the good overall charge neutralisation by the positive ions of the secondary plasma. It demonstrates the perfect compensation of the space charge induced by the secondary plasma (Fig. 3 (a) – red zone). The halo of early neutralised particles follows almost parallel trajectories (Fig. 3 (a) – blue zone) since they are not any longer affected by the space charge or electric field.

The stripped electrons follow the beam, but they can also hit the neutraliser walls (Fig. 3 (b), blue region ) and fill the space between the neutraliser and the RID (Fig. 3 (b) ;  $z > 5$ m). The first stripped electrons appear before the entry plane of the neutraliser due to the collisions between the beam particles and the residual target gas (Fig. 3 (b) at  $z \sim 2$  m).

As mentioned above, the plasma particle densities are higher than the beam ones, so one can expect some of them flowing rearward the beam. That is the case for the positive ions leaving the neutraliser through the entry plane (Fig. 3 (c) , red region  $1$  m  $< z < 2$  m). This flow of positive plasma ions goes to the accelerator. Assuming only one large aperture of 100 mm diameter in the final accelerator grid (analogous to SINGAP structure), about a half of these ions hit the acceleration grid, while the other half penetrate the grid aperture and can be accelerated towards the negative ion source.

At the other end of the neutraliser both ions and electrons diffuse close to the walls and fill the space between the neutraliser and the RID (Fig. 3 (c) and (d) ,  $z > 5$  m).

Both types of electrons, stripped and plasma electrons, have a significant contribution to the ionisation of the gas molecules as can be seen from Figure 4, which shows that the ionisation rate of the plasma electrons is twice larger than the ionisation due to stripped electrons. Simulations show that the secondary plasma contribution increases with the number of beamlets composing the beam, at least in a 2D( $r,z$ ) geometry.

Concerning the plasma potential (not shown), its maximum value is  $\sim 12$  V (at  $z = 3.7$  m and on the axis) and it smoothly decreases when moving away along the neutraliser axis.

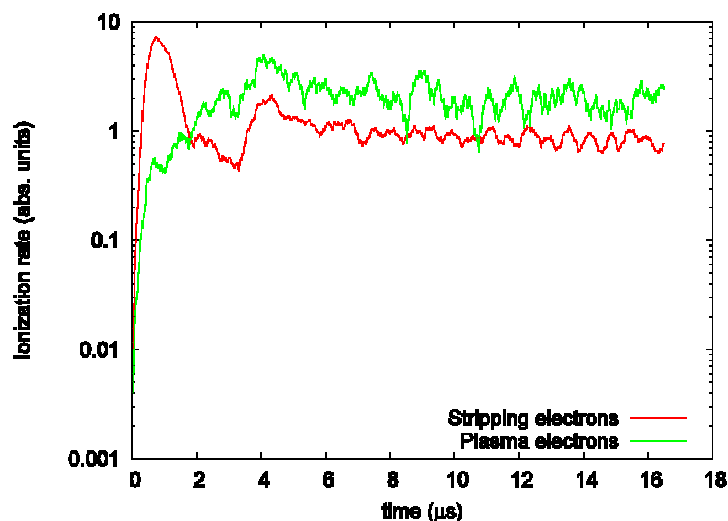


Figure 4 – Ionisation rate induced by the stripped electrons and secondary plasma electrons for the broad beam (80 mm diameter)

## 4. Conclusion

We have presented the results obtained with new developed OBI-2 code. Both the volume processes and particle-wall interaction were analysed within a simplified kinetic scheme. Considering the secondary plasma density, we obtain the same order of magnitude as E. Surrey [5], but with a smaller value for the mean electron energy ( $\sim 10$  eV) compared to her estimation ( $\sim 40$  eV).

Present results are restricted to the case a broad homogeneous beam (80 mm diameter) equivalent to  $\sim 10$  beamlets. From the present calculations, which consider a larger volume ranging from the acceleration grid to the RID entrance, the following physical conclusions have been drawn.

i) The plasma density inside the neutraliser is large enough to induce a field that can affect the transport of the beam. In particular, the beam spatial charge is screened after  $\sim 10$   $\mu$ s, by the positive space charge of the secondary plasma. This effect drastically reduces the beam divergence at the exit plane; ii) The residual target gas density in the space between the accelerating grids has to be taken into account. Ionisation processes occurring in this region produce a halo around the beam even when the injected beam emittance is zero; iii) The role of the ionisation processes induced by the secondary plasma electrons was underlined and for high currents it is the dominant process with respect to the ionisation by the stripped electrons; iv) The acceleration field leakage through the final acceleration grid aperture contributes significantly to setting of a plasma ion flow into the accelerator.

Our results clearly demonstrate that the possible expansion of the secondary plasma outside the neutraliser and its influence on the beam transport is an important issue that should be addressed in detail. Quantitative prediction about the plasma flow needs to consider 3D geometries. This is the main objective for the next step of our modelling.

## References

- [1] J.-L. Vay, C. Deutsch, in: E. Panarella (Ed.), *Current Trends in International Fusion Research—Proceedings of the Third Symposium, Canada, 2002*; J.-L. Vay, Ph. D. Thesis, Université Paris-Sud, Orsay (1996) (*in French*)
- [2] A. Lifschitz, G. Maynard, J.-L. Vay, *Nuclear Instruments and Methods in Physics Research A* 544 (2005) 202–209
- [3] Birdsall, C. and Langdon, A. *Plasma Physics via Computer Simulation* Mc Graw Hill, New York (1995)
- [4] T. Minea, A. Lifschitz, G. Maynard, K. Katsonis, J. Bretagne, A. Simonin, *Journal of Optoelectronics and Advanced Materials*, **10**, (2008), 1899
- [5] E. Surrey, *Nucl. Fusion*, **46** (2006) S360-S368
- [6] IAEA AMDIS ALADDIN Database: [www-amdis.iaea.org/ALADDIN/](http://www-amdis.iaea.org/ALADDIN/)
- [7] R.K. Janev, D. Reiter, U. Samm, “Collision Processes in Low-Temperature Hydrogen Plasmas”, Rapport EIRENE: [www.eirene.de/](http://www.eirene.de/)
- [8] T. Simko, PhD. Thesis, Université Paris Sud, France (1997) (*in French*)
- [9] F. Duré, A. Lifschitz, G. Maynard, K. Katsonis, J. Bretagne, A. Simonin, T. Minea, AIP Conference Proceedings, 1st International Conference on Negative Ions, Beams and Sources - NIBS 2008 - Sept. 10-12, 2008, Aix en Provence, France.
- [10] M. Dremel, EFDA - CCNB meeting, Culham, 22 to 24 May 2007